Afterglow Properties of Silica-Capped $Sr_2MgSi_2O_7$:Eu,Dy Nanoparticles Prepared by Laser Ablation in Ethanol

M. Ishizaki, T. Fuchigami, T. Katagiri, T. Sasagawa, Y. Kitamoto, O. Odawara, H. Wada*

Tokyo Institute of Technology, 4259 Nagatsuta-cho, Midori-ku, Yokohama 226-8503 Japan.

**Correspondence author*, E-mail: wada.h.ac@m.titech.ac.jp

doi:10.5618/chem.2012.v2.n1.6 || Received: 20-10-2012, Accepted: 01-11-2012, Available online: 06-11-2012

Abstract

The effect of silica-capping on the afterglow property of $Sr_2MgSi_2O_7$:Eu,Dy nanoparticles was investigated. $Sr_2MgSi_2O_7$:Eu,Dy nanoparticles were prepared by laser ablation in liquid. Afterglow nanoparticles were capped with silica using Stöber method. A dense silica capping layer was achieved after 4 hours of reaction. Silica-capping of the afterglow nano-particles improved the particles' afterglow property, which was degraded by nanosizing. Decay curves indicated that initial values of afterglow intensity were increased with silica-capping capacity. Moreover, silica-capping decreased the decay curve constant γ, which was related to trap parameters. The decrease in the value of γ resulted in the reduction in the slope of decay curve, and thus the improvement of the afterglow property. We concluded that capping nanoparticles with silica improved the particles' afterglow property by the passivation of surface defects and the prevention of energy transfer to water molecules.

Keywords: Afterglow; Nanoparticle; SiO_2; Laser ablation.

1. Introduction

Extensive studies have recently been conducted regarding afterglow materials because of their unique optical properties and various potential applications, such as security and operability in the dark. Since the afterglow material $SrAl_2O_4$,Eu,Dy, which does not feature radioactive materials, was discovered in 1996, it has been used in the faces of watches [1]. The afterglow mechanism, which involves the recombination of electrons and holes trapped in shallow energy levels at room temperature, has been extensively studied [1-6]. $Sr_2MgSi_2O_7$:Eu,Dy is known to be a water-insoluble afterglow material [7-9].

Nanomaterials are also widely studied due to their promising physical properties. The nanosizing of afterglow materials would expand their application in various fields. We believe that $Sr_2MgSi_2O_7$:Eu,Dy will be useful in bioimaging to reduce the problem of autofluorescence. Nanoparticles are produced using various methods. One promising method is laser ablation in a liquid [10-12]. $Sr_2MgSi_2O_7$:Eu,Dy nanoparticles have been successfully formed by this method [13]. However, the optical properties of $Sr_2MgSi_2O_7$:Eu,Dy nanoparticles are degraded due to nanosizing. This aspect has been improved upon by surface passivation with polyethylene glycol (PEG) [14]. However, the long-term stability of organic materials is still not adequate for practical use because PEG molecules are simply adsorbed onto the surfaces of nanoparticles.

The nanosizing of materials increases particles' specific surface area. Many defects exist on the surface and adversely affect the optical properties of particles by nonradiative relaxation through the energy levels of surface defects and/or energy transfer to water molecules [13,15]. Silica-capping is one of the most effective ways of passivating the surfaces of nanoparticles and improving their optical properties [16]. The Stöber method has been widely studied as a silica-capping technique; it involves hydrolysis and condensation reactions [17]. Capping nanoparticles with silica proceeds by the reaction between tetraethyl orthosilicate (TEOS) and water through heterogeneous nucleation, while the formation of silica nanoparticles proceeds through homogeneous nucleation.

In this study, afterglow nanoparticles of $Sr_2MgSi_2O_7$:Eu,Dy prepared by laser ablation in liquid were capped with a stable inorganic material, silica. The afterglow properties of the nanoparticles were improved by silica-capping.

2. Materials and Methods

2.1. Materials. A powder of the water-insoluble afterglow material, $Sr_2MgSi_2O_7$:Eu,Dy, was purchased from Mitsubishi Chemical. Ethanol, 1-propanol,

tetraethyl orthosilicate and ammonia solution were purchased from Kanto Chemical. These reagents were not further purified.

2.2. Preparation of afterglow nanoparticles. First, the target for laser ablation in liquid was fabricated as follows. The powder of the afterglow material was pressed in a stainless steel mold. This pellet was sintered in an electric furnace at 1100 °C for 1 hour. Argon was flowed into the tube of the furnace to prevent the oxidation of Eu^{2+}. Second, afterglow nanoparticles were prepared by laser ablation in liquid. The target was placed in a cuvette in air. It was irradiated with a focused Nd:YAG laser beam (third harmonic generation, THG) in ethanol for 6 hours. The laser was a model M210 instrument (JDSU, wavelength: 355 nm, repetition rate: 7 kHz, pulse duration 50 ns). The focal length of the lens was 90 mm. The energy density of the laser beam on the top of the target was adjusted by varying the diameter of the laser beam.

2.3. Capping afterglow nanoparticles with silica. The silica-capping of nanoparticles was performed by the Stöber method. TEOS and ammonia water were added to a solution containing the nanoparticles of one batch production of laser ablation. The capping reaction proceeded under ultrasonication. The temperature of the solution was held at 20 °C. The reaction time of this process was varied. The reaction was ceased by the addition of 1-propanol.

2.4. Characterization. The X-ray diffraction (XRD) pattern of the particles was measured using an X-ray diffractometer (Bruker, D8 Discover μHR). A silica-coated nanoparticle was observed by transmission electron microscopy (TEM, Hitachi High-Technologies, H-8100). The nanoparticle-dispersed solution was dropped onto a carbon membrane on a copper grid, and water was removed by drying in a vacuum oven. The optical properties of the silica-capped nanoparticles were investigated by fluorescence spectrometry (Hitachi High-Technologies, F-7000).

3. Results and Discussion

The XRD pattern of the target is shown in **Figure 1**. It corresponds to that of $Sr_2MgSi_2O_7$. It indicates no transformation of the host material during heating for target fabrication. The photoluminescence (PL) spectrum of the target also corresponds to that of the sample powder. These results indicate no transformation of the luminescent center, Eu^{2+}.

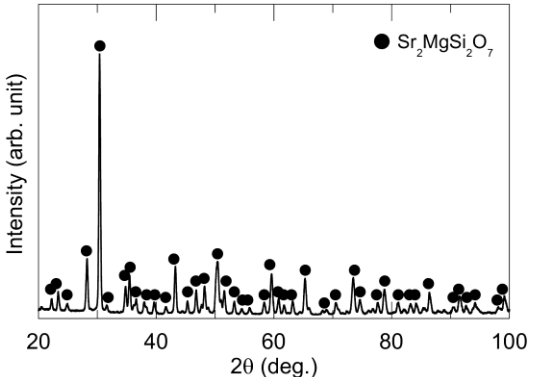

Fig. 1. XRD spectra of the target.

Figure 2 shows TEM images of the silica-capped nanoparticles. The dark portion would indicate the afterglow nanoparticles. The shape of silica in **Figure 2a** (reaction time: 1 hour) was rod-like, while that in **Figure 2b** (reaction time: 4 hours) was densely packed. After a capping reaction time of 4 hours, a silica-capping layer would closely adhere to the surface of the nanoparticles and be able to protect the particles against water molecules. **Figure 2c** shows a high-magnification image of the silica-capped nanoparticles. The afterglow nanoparticles were completely covered with a silica layer.

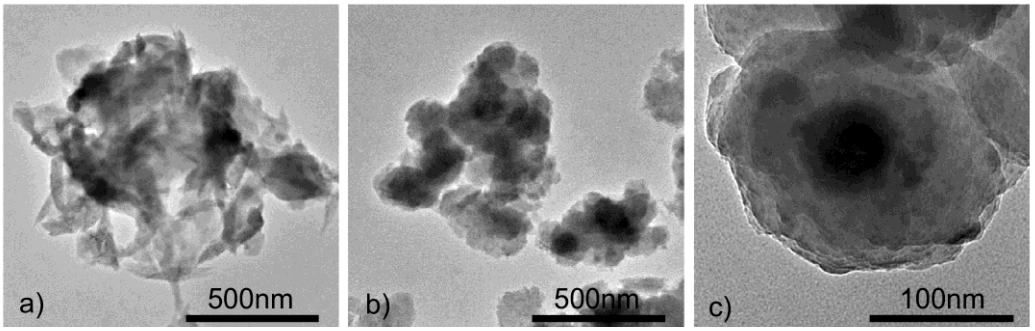

Fig. 2. TEM images of silica-capped nanoparticles. Silica-capping reaction time: a) 1 hour (low magnification), b) 4 hours (low magnification) and c) 4 hours (high magnification).

The PL spectrum of the afterglow nanoparticles in ethanol is shown in **Figure 3**. A broad, strong peak at approximately 466 nm is attributed to the 3d transition of Eu^{2+}, which was sensitive to the host material. This peak corresponds to the luminescence of the target. Second-order scattering of excitation (276 nm) was observed at approximately 560 nm. A weak peak at approximately 607 nm is also shown in **Figure 3**. The emission in the vicinity of 600 nm is due to the magnetic dipole transition $^5D_0 \rightarrow {}^7F_1$, which is insensitive to the site symmetry [18]. The emission at approximately 610-630 nm is due to the electric dipole transition $^5D_0 \rightarrow {}^7F_2$, which is induced by the lack of inversion symmetry of the Eu^{3+} site and is much stronger than that of the transition to the $^7F_1$ state [18]. The peak at approximately 607 nm in **Figure 3** is related to the electric dipole transition of Eu^{3+} because the crystal structure of $Sr_2MgSi_2O_7$ is tetragonal with space group $P42_1m$ (No. 113) [19]. Eu^{2+} in the $Sr_2MgSi_2O_7$ matrix would slightly be oxidized by the thermal effect of laser ablation in ethanol. However, the PL properties of the nanoparticles mainly depend on the Eu^{2+} ions, much like the target.

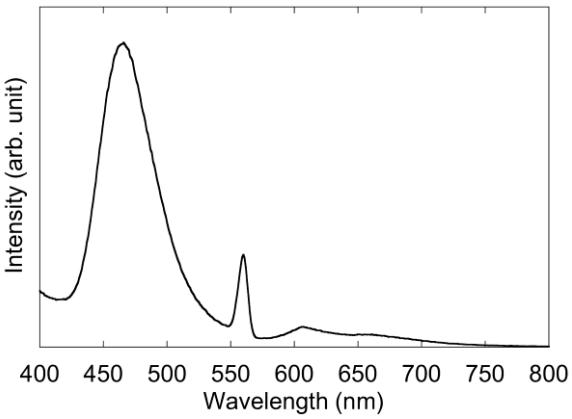

Fig. 3. PL spectrum of afterglow nanoparticles of $Sr_2MgSi_2O_7$:Eu,Dy at an excitation wavelength of 276 nm.

The effect of the Stöber method reaction time on the afterglow properties of the nanoparticles is illustrated in **Figure 4**. The reaction time varied from 0 to 4 hours. The decay curves plot the afterglow intensity as a function of time after blocking the excitation. The afterglow property obeys the following equations [20]:

$$I_{(t)} = I_0 / (1+\gamma t)^n , \qquad (1)$$

$$\gamma = N / an_t , \qquad (2)$$

where the afterglow intensity is $I_{(t)}$, the initial value is I_0, time is t, the trap concentration is N, the probability that a trapped carrier will be thermally led into the band is a and the number of carriers per unit volume in the trap level is n_t. The data in **Figure 4** was fitted as indicated by the solid lines. **Figure 5** plots the initial values of equation (1) I_0 as a function of the reaction time. The initial value I_0 increased with increasing reaction time. The differences among the decay curves in **Figure 4** mainly depended on the difference between the initial values I_0. The constant γ, which is related to the trap concentration N, indicates the probability that a trapped carrier will be thermally led into the band a, and the number of carriers per unit volume in the trap level n_t determines the slope of the decay curve during the initial stage. The slope is steep if γ is large, while the slope is gentle if γ is small. **Figure 6** shows the value γ of equation (1) as a function of the reaction time. At a capping reaction time of 0 hour (without capping), the value γ is large, which indicates fast decay. However, at a capping reaction time of 4 hours, the value γ is small, which indicates slow decay. Both parameters I_0 and γ indicated that a long capping reaction time improved the afterglow property of the nanoparticles. A valid mechanism of the degradation of the afterglow property would be deactivation through surface defects and/or energy transfer to water molecules. TEM observation indicated that a long capping reaction time could allow for the dense capping of the nanoparticle surfaces with silica. The dense capping layer would passivate the surface defects and prevent energy transfer to water molecules. Therefore, long capping reaction times led to a significant improvement in the afterglow property of the nanoparticles.

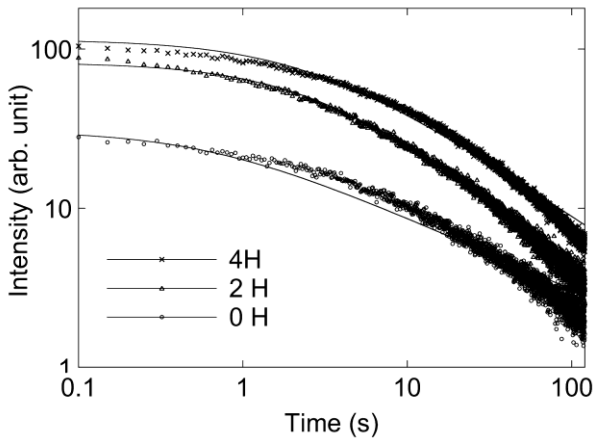

Fig. 4. Afterglow properties of silica-capped nanoparticles. The reaction time varied from 0 to 4 hours.

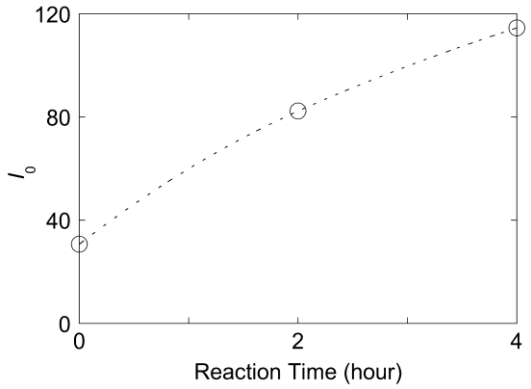

Fig. 5. Afterglow parameter I_0 as a function of the silica-capping reaction time.

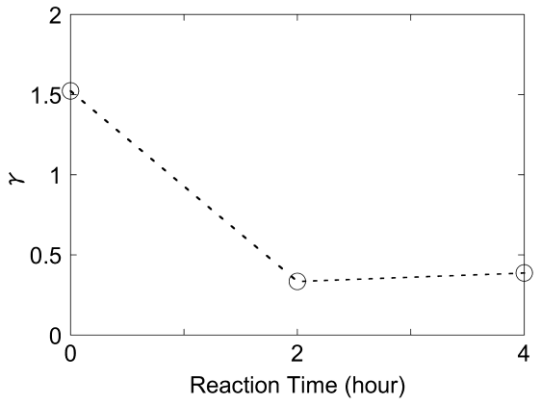

Fig. 6. Afterglow parameter γ as a function of the silica-capping reaction time.

4. Conclusion

Afterglow nanoparticles of $Sr_2MgSi_2O_7$:Eu,Dy were prepared by laser ablation in ethanol. They were capped with silica by using the Stöber method. Silica-capping improved the afterglow property of the nanoparticles. The increase in reaction time of silica-capping led to the dense capping of nanoparticles. In general, the non-radiative relaxation through surface defects, and the energy transfer from surface to water molecules reduce optical properties. Surface passivation such as capping decreases the influences and improves optical properties usually. Therefore, the initial value and the slope of afterglow properties were improved. We concluded that the capping layer passivates surface defects and prevents energy transfer to water molecules, thus improving the afterglow property of the nanoparticles.

Acknowledgement

We thank H. Iida and Y. Suzuki at the Center for Advanced Materials Analysis, Tokyo Tech. This study was supported by JSPS KAKENHI Grant.

References

[1] T. Matsuzawa, Y. Aoki, N. Takeuchi, Y. Murayama, J. Electrocem. Soc. 143 (1996) 2670-2673. http://dx.doi.org/10.1149/1.1837067

[2] A.A. Setlur, A.M. Srivastava, H.L. Pham, M.E. Hannah, U. Happek, J. Appl. Phys. 103 (2008) 053513-053518. http://dx.doi.org/10.1063/1.2844473

[3] M. Yamaga, Y. Tanii, N. Kodama, T. Takahashi, M. Honda, Phys. Rev. B, 65 (2002) 235108-235118. http://dx.doi.org/10.1103/PhysRevB.65.235108

[4] T. Kinoshita, M. Yamazaki, H. Kawazoe and H. Hosono, J. Appl. Phys. 86 (1999) 3729-3733. http://dx.doi.org/10.1063/1.371243

[5] J. Qiu, A. Makishima, Sci. Tech. Adv. Mater. 4 (2003) 35-38. http://dx.doi.org/10.1016/S1468-6996(03)00008-1

[6] M. Yamaga, N. Kodama, J. Alloys Comp. 408-412 (2006) 706-710. http://dx.doi.org/10.1016/j.jallcom.2005.01.092

[7] Q. Fei, C. Chang, D. Mao, J. Alloys Comp. 390 (2005) 133-137. http://dx.doi.org/10.1016/j.jallcom.2004.06.096

[8] Y. Chen, B. Liu, M. Kirm, Z. Qi, C. Shi, M. True, S. Vielhauer, G. Zimmerer, J. Lumin. 118 (2006) 70-78. http://dx.doi.org/10.1016/j.jlumin.2005.05.011

[9] A.R. Mirhabibi, F. Moztarzadeh, A.A. Bazazi, M. Solati, A. Maghsoudipour, M.H. Sarrafi, Pigment Resin Tech. 33 (2004) 220-225. http://dx.doi.org/10.1108/03699420410546908

[10] J. Neddersen, G. Chumanov, T. Cotton, Appl. Spectrosc. 47 (1993) 1959-1964. http://dx.doi.org/10.1366/0003702934066460

[11] A. Fojtik, A. Henglein, Ber. Bunsen-Ges. Phys. Chem. 97 (1993) 252-254. http://dx.doi.org/10.1002/bbpc.19930971112

[12] F. Mafune, J. Y. Kohno, Y. Takeda, T. Kondow, H. Sawabe, J. Phys. Chem. B 104 (2000) 8333-8337. http://dx.doi.org/10.1021/jp001803b

[13] F. Yoshimura, K. Nakamura, F. Wakai, M. Hara, M. Yoshimoto, O. Odawara, H Wada, Appl. Surf. Sci. 257 (2011) 2170-2175. http://dx.doi.org/10.1016/j.apsusc.2010.09.067

[14] F. Yoshimura, M. Ishizaki, F. Wakai, M. Hara, O. Odawara, H. Wada, Adv. Opt. Tech. 2012 (2012) 814745. http://dx.doi.org/10.1155/2012/814745

[15] F. Wang, J. Wang, X. Liu, Angew. Chem. Int. Ed. 49 (2010) 7456 –7460. http://dx.doi.org/10.1002/anie.201003959

[16] H. Takahashi, T. Isobe, Jpn. J. Appl. Phys. 44 (2005) 922–925. http://dx.doi.org/10.1143/JJAP.44.922

[17] W. Stöber, A. Fink, E. Bohn, J. Coll. Interface Sci. 26 (1968) 62–69. http://dx.doi.org/10.1016/0021-9797(68)90272-5

[18] T. Kano, in: W.M. Yen, S. Shionoya, H. Yamamoto (Eds.), Phosphor Handbook, CRC Press, Boca Raton, 2006, Chapter 3.3.

[19] M. Kimata, Z. Kristallogr. 163 (1983) 295-304. http://dx.doi.org/10.1524/zkri.1983.163.3-4.295

[20] E. Nakazawa, in: W.M. Yen, S. Shionoya, H. Yamamoto (Eds.), Phosphor Handbook, CRC Press, Boca Raton, 2006, Chapter 2.7.